View metadata, citation and similar papers at core.ac.uk

brought to you by CORE

provided by Elsevier - Publisher Connector

Biochimica et Biophysica Acta 1838 (2014) 1693–1700

Contents lists available at ScienceDirect

Biochimica et Biophysica Acta

journal homepage: www.elsevier.com/locate/bbamem

Biochemical characterization of sporadic/familial hemiplegic migraine mutations

Karl M. Weigand [a], Herman G.P. Swarts [b], Frans G.M. Russel [a], Jan B. Koenderink [a,*]

[a] Department of Pharmacology and Toxicology 149, Radboud University Medical Centre, P.O. Box 9101, 6500 HB Nijmegen, The Netherlands
[b] Department of Biochemistry 286, Radboud University Medical Centre, P.O. Box 9101, 6500 HB Nijmegen, The Netherlands

ARTICLE INFO

Article history:
Received 15 November 2013
Received in revised form 26 March 2014
Accepted 27 March 2014
Available online 3 April 2014

Keywords:
Na^+,K^+-ATPase
ATP1A2
Familial hemiplegic migraine
FHM2
Alpha 2 isoform
Baculovirus expression system

ABSTRACT

Sporadic hemiplegic migraine type 2 (SHM2) and familial hemiplegic migraine type 2 (FHM2) are rare forms of hemiplegic migraine caused by mutations in the Na^+,K^+-ATPase α2 gene. Today, more than 70 different mutations have been linked to SHM2/FHM2, randomly dispersed over the gene. For many of these mutations, functional studies have not been performed. Here, we report the functional characterization of nine SHM2/FHM2 linked mutants that were produced in *Spodoptera frugiperda* (Sf)9 insect cells. We determined ouabain binding characteristics, apparent Na^+ and K^+ affinities, and maximum ATPase activity. Whereas membranes containing T345A, R834Q or R879W possessed ATPase activity significantly higher than control membranes, P796S, M829R, R834X, del 935–940 ins Ile, R937P and D999H membranes showed significant loss of ATPase activity compared to wild type enzyme. Further analysis revealed that T345A and R879W showed no changes for any of the parameters tested, whereas mutant R834Q possessed significantly decreased Na^+ and increased K^+ apparent affinities as well as decreased ATPase activity and ouabain binding. We hypothesize that the majority of the mutations studied here influence interdomain interactions by affecting formation of hydrogen bond networks or interference with the C-terminal ion pathway necessary for catalytic activity of Na^+,K^+-ATPase, resulting in decreased functionality of astrocytes at the synaptic cleft expressing these mutants.

© 2014 Elsevier B.V. All rights reserved.

1. Introduction

The Na^+,K^+-ATPase is a cation-transporting membrane protein involved in active transport of sodium and potassium ions against their concentration gradients across the cell membrane. For every molecule of ATP consumed, three sodium ions are exported from the cell in exchange for import of two potassium ions. The Na^+,K^+-ATPase serves many roles, including cell-volume homeostasis as well as maintenance of the membrane potential. In addition, the generated Na^+ and K^+ gradients drive various secondary active transporters. Since transport of Na^+ and K^+ across the cell membrane takes place against such steep concentration gradients, the enzyme consumes high amounts of energy: approximately 25–50% of cellular ATP is consumed by the Na^+,K^+-ATPase [1,2].

The Na^+,K^+-ATPase consists of at least two different subunits: an α-subunit (110 kDa), containing ten transmembrane α-helices (αM1–αM10) and two large cytosolic loops (αM2–αM3 and αM4–αM5), together with a highly glycosylated single transmembrane domain spanning β-subunit (50 kDa). In some tissues, a third subunit containing a characteristic FXYD motif is present as well (γ-subunit) [3]. In the human genome, four α-subunit encoding genes have been described. The proteins encoded by these genes share a sequence homology of approximately 80–90% and are expressed tissue specifically [4]. For example, the α1-isoform is expressed ubiquitously [5], whereas the α4-isoform is detected only in the testis [6]. The α3-isoform is present in both the central and peripheral nervous systems [7,8], whereas the α2-isoform is expressed in different tissues including heart skeletal muscle, vascular smooth muscle, bone, adipocytes, and astrocytes [9].

Genetic studies have linked over 70 mutations in the *ATP1A2* gene (chromosome 1q23) encoding the α2-isoform of the Na^+,K^+-ATPase to sporadic/familial hemiplegic migraine type 2 (SHM2/FHM2), shown in Fig. 1 [10]. Sporadic (only one affected family member) and familial (two or more affected family members) hemiplegic migraine are autosomal-dominant monogenic subtypes of migraine with aura (MA), characterized by neurological aura symptoms preceding the migraine attack. In addition to the mutations present in the α2-isoform of Na^+,K^+-ATPase, two other genes have been linked to FHM: *CACNA1A* has been linked to SHM1/FHM1 whereas *SCN1A* has been associated with FHM3 (no sporadic mutations reported) [11]. Together, SHM and FHM show a prevalence of approximately 0.005% [12,13].

The exact pathophysiology of SHM2/FHM2 remains to be elucidated, but it is assumed that α2-isoform Na^+,K^+-ATPase mutations result in

* Corresponding author. Tel.: +31 24 36 13654; fax: +31 24 36 14214.
E-mail addresses: Karl.Weigand@radboudumc.nl (K.M. Weigand), H.Swarts@ncmls.ru.nl (H.G.P. Swarts), Frans.Russel@radboudumc.nl (F.G.M. Russel), Jan.Koenderink@radboudumc.nl (J.B. Koenderink).

http://dx.doi.org/10.1016/j.bbamem.2014.03.022
0005-2736/© 2014 Elsevier B.V. All rights reserved.

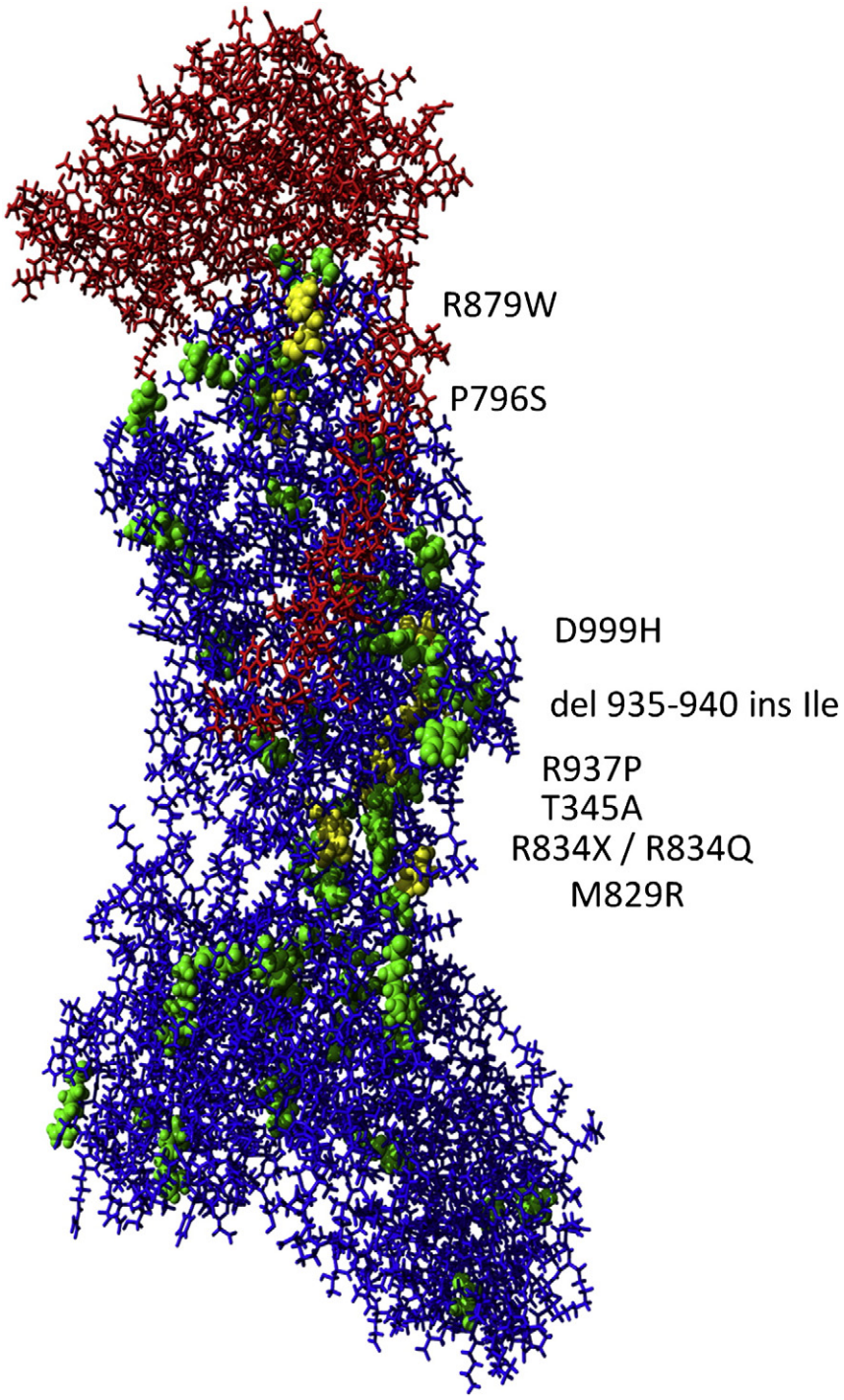

Fig. 1. Homology model of the α2-isoform of Na^+,K^+-ATPase (based on PDB ID: 2ZXE [38]) showing the residues that are associated with SHM2/FHM2 mutations in literature highlighted in green, whereas the mutations described in the present study are highlighted in yellow. The α-subunit is shown in blue, whereas red represents the β-subunit: these two subunits together constitute a functional Na^+,K^+-ATPase.

altered enzyme functionality at the synaptic cleft, where astrocytes expressing the α2-isoform are present as supporting cells. The Na^+, K^+-ATPase present at the plasma membrane of these cells presumably plays a role in uptake of K^+ from the synaptic cleft following nerve excitation, resulting in a favorable driving force for the re-uptake of glutamate by the co-localized glutamate transporter [14]. Changes in the enzymatic properties of the Na^+,K^+-ATPase might therefore have an indirect effect on signal transmission via the synaptic cleft, leading to hemiplegic migraine attacks.

Over 70 SHM2/FHM2 causing mutations in the *ATP1A2* gene have been reported, randomly dispersed over the gene [15]. For many of these mutations the effects on enzyme functionality have not been reported yet, whereas investigation of the biochemical effects of each of these mutations on protein functionality is an essential step towards understanding the pathogenesis of SHM2/FHM2 mutations. Using *Spodoptera frugiperda* (Sf)9 insect cells lacking endogenous Na^+,K^+-ATPase, we set out to characterize the enzymatic effects of nine SHM2/FHM2 mutations (all except T345A) located within the

carboxy-terminal transmembrane segment: T345A, P796S, M829R, R834Q, R834X (truncated protein), R879W, del 935–940 ins Ile, R937P and D999H. The carboxy-terminal segment is present only in PII- and PIIIa-type ATPases of the P-type ATPase family [16]. It plays a vital role in the catalytic activity of the Na^+,K^+-ATPase as was illustrated by the discovery of an essential C-terminal half-channel forming a gateway to the third ion-binding site, allowing protons to access the third ion-binding site as required for K^+ occlusion [17]. Interestingly, various SHM2/FHM2 mutations have been mapped to this half-channel, leading us to investigate extensively the biochemical effects of mutations located within this region of the Na^+,K^+-ATPase.

2. Methods

2.1. The Gateway system

The cDNA for the α2-isoform was obtained by purchasing a vector (Thermo Scientific MHS1011-9199751) containing the cDNA obtained from a human teratocarcinoma cell line (cDNA: NM_000702). The desired mutations were obtained by performing two PCRs (A and B) on human Na^+,K^+-ATPase α2 wild type cDNA using either a 5′ or a 3′ primer together with a mutagenesis primer (Biolegio, Nijmegen, The Netherlands) containing the desired mutation (see Supplementary Table 1). This resulted in generation of two fragments that were subsequently combined in a PCR (C) using only the 5′ and 3′ primers, allowing for annealing of the two fragments. Using Gateway cloning (Life Technologies, Breda, The Netherlands), the mutated Na^+,K^+-ATPase α2 gene was then transferred to an entry vector containing a kanamycin resistance cassette using BP Clonase II enzyme according to the manufacturer's instructions. After successful transformation of entry clones into *Escherichia coli* DH5α cells and overnight selection on kanamycin LB-agar plates, colonies were inoculated in LB medium containing kanamycin, grown overnight and subsequently isolated using the GenElute™ mini-prep isolation kit (Sigma-Aldrich). Then, full-length sequencing of the different constructs was performed to check for successful mutagenesis. Subsequently, expression clones were obtained by inserting the α2 gene carrying the mutation in the Gateway Reading Frame Cassette B behind a polyhedrin promoter in an ampicillin resistant pFastBac Dual transfer vector containing the β1-subunit behind the p10 promoter using LR Clonase II enzyme (Life Technologies, Breda, The Netherlands). After successful transformation of expression clones into *E. coli* DH5α cells and overnight selection on ampicillin LB-agar plates, colonies were inoculated in LB medium containing ampicillin, grown overnight and subsequently isolated using the GenElute™ mini-prep isolation kit (Sigma-Aldrich). Throughout the cloning procedures, YFP was used as a negative control, resulting in the generation of an expression clone encoding YFPβ1.

2.2. Generation of recombinant baculoviruses

The expression clones generated using the Gateway system were transformed to competent DH10Bac *E. coli* cells (Life Technologies, Breda, The Netherlands) harboring the baculovirus genome (bacmid) and a transposition helper plasmid, conferring resistance against kanamycin, gentamycin, and tetracycline. Upon transposition between the Tn7 sites present in both bacmid and expression clones [18], recombinant bacmids were selected on LB-agar plates containing kanamycin, gentamycin, and tetracycline. Subsequently, resistance-selected bacmids were transfected to *S. frugiperda* (Sf)9 insect cells grown in Grace medium (Sigma, Bornem, Belgium) at 27 °C in 175 cm^2 monolayers using Cellfectin reagent (Life Technologies, Breda, The Netherlands). After a 6-day period, recombinant baculoviruses were harvested and used to infect fresh Sf9 cells at a multiplicity of infection of 0.1 [19]. After another 6 days of culture of infected Sf9 cells, amplified baculoviruses were harvested [20].

2.3. Protein production using recombinant virus

Sf9 cells grown at 27 °C in 175 cm^2 monolayers and later in 500 mL shaking flasks in Xpress medium (Sigma, Bornem, Belgium) were infected at a density of $1.5 \cdot 10^6$ cells mL^{-1} in the presence of 1% (v/v) ethanol as described before [21]. After three days of infection, the cells were harvested by centrifugation at 2000 ×*g* for 5 min. Then, the pelleted cells were resuspended at 0 °C in a 0.25 M sucrose, 2 mM EDTA and 20 mM Hepes/Tris (pH 7.0) buffer. Sonication was performed for 30 s at 80 W prior to centrifugation at 10,000 ×*g* at 4 °C for 30 min, followed by centrifugation of the resulting supernatant at 100,000 ×*g* at 4 °C for 60 min. The pelleted membranes were resuspended using the buffer mentioned above, homogenized and stored at −20 °C and the protein concentration was determined using the modified Lowry method [22].

2.4. Western blotting

Approximately 10 μg of membranes was treated with SDS-PAGE solubilization buffer overnight at room temperature before loading on a 10% polyacrylamide gel, as described previously [23]. After separation, the proteins were transferred overnight to a nitrocellulose membrane at 30 V. The alpha and beta subunits were detected using either the C356-M09 (α-subunit) or the C385-M77 (β-subunit) antibodies, respectively [21,23].

2.5. Ouabain binding experiments

Ouabain binding was determined by incubation of approximately 150–200 μg of membranes in the presence of 20 mM histidine, 5 mM $MgCl_2$, 5 mM H_3PO_4 pH 7.0 and 25 nM of radiolabeled ouabain (Perkin-Elmer, Waltham, MA, USA) in a final volume of 60 μL at room temperature for 2 h. After incubation for 15 min on ice, the amount of bound ouabain was determined by washing the samples over a 0.8 μm ME27 filter using distilled H_2O, retaining the enzyme-bound ouabain to the filters. The amount of radioactivity on the filters was then determined in a liquid scintillation counter after addition of 4 mL OptiFluor (Canberra Packard, Tilburg, The Netherlands) [24]. Correction for endogenous ouabain binding was performed by subtracting the amount of ouabain bound in YFPβ1 samples.

2.6. ATPase activity studies

ATPase activity was determined in the Na^+ or K^+ affinity studies by incubating 20 μL of membranes in a final volume of 100 μL containing 50 mM Tris–Ac pH 7.0, 0.1 mM EGTA, 1.2 mM $MgCl_2$, 1.0 mM Tris–N_3, and 100 μM of radiolabeled ATP in the presence of 50 mM NaCl or 5.0 mM KCl and increasing concentrations of KCl or NaCl, respectively. After incubation of the samples for 30 min at 37 °C, the reaction was stopped by addition of 500 μL 10% (w/v) charcoal in 6% (v/v) trichloroacetic acid and, after 10 min at 0 °C, the mixture was centrifuged for 30 s (10,000 ×*g*). Subsequently, 150 μL of the clear supernatant was mixed with 4 mL OptiFluor before analysis using a liquid scintillation counter to determine the amount of formed P_i (inorganic phosphate), a measure of ATPase activity [25]. Na^+,K^+-ATPase specific activity was determined by subtracting the amount of P_i formed in the presence of 1.0 mM ouabain. [γ-^{32}P]ATP (3000 Ci $mmol^{-1}$) was obtained from Perkin-Elmer (Waltham, MA, USA).

2.7. Data analysis

All data were analyzed using GraphPad Prism 5.02. Repeated measures ANOVA was used to test for differences in apparent Na^+ and K^+ affinities and maximum ATPase activity levels compared with α2 wild type enzyme, with $\alpha = 0.05$. Ouabain binding characteristics (maximum ouabain binding (EO_{max}) and K_d) were tested for differences

compared to wild type enzyme using Student's *t*-test. With regard to the Na^+ and K^+ affinities the Origin 6.1 (Microcal, Northampton, MA) software was used to perform non-linear regression analysis. The $Na^+_{0.5}$ and $K^+_{0.5}$ values (defined as the concentrations of Na^+ and K^+ resulting in half-maximal activation) were calculated via the Hill equation using the averaged data and SEM values, and the Hill coefficients (nH) obtained for wild type Na^+,K^+-ATPase were also used for calculation of the mutant half-maximum Na^+ and K^+ concentrations. Maximum ATPase activity was determined in the presence of 50 mM NaCl, 5.0 mM KCl, 1.2 mM $MgCl_2$ and 0.1 mM ATP at pH 7.0.

2.8. Structural analysis

Homology models based on different crystal structures of the α1β1 Na^+,K^+-ATPase (enzyme obtained from pig and shark) and sarcoplasmatic reticulum Ca^{2+}-ATPase (SERCA) were used as templates to investigate the possible interactions between residues of interest using the YASARA software. The following PDB entries were used (corresponding enzyme conformation): 2C9M (E_1Na^+), 1T5S (E_1Na^+-ATP), 1T5T (E_1Na^+-P-ADP), 3BA6 (E_1Na^+P:ADP), 3B9B (E_2P), 3B9R (E_2K^+-P-ATP), 2ZXE ($E_2.K^+.P_i$), and 2C88 (E_2K^+ ATP). The homology models were built using the YASARA software and the WHAT IF Twinset using default parameters. YASARA-calculated Z-scores were used for validation and selection of the best model and ranged from −1.990 (3B9R), −1.788 (3B9B), −1.762 (2C9M), −1.699 (1T5T), −1.644 (3BA6), −1.557 (2C88), −1.548 (1T5S) to −0.454 (2ZXE). Minimization was performed using an automatic YASARA protocol and default settings [26].

3. Results

3.1. General characterization of ATP1A2 migraine mutants

We selected 9 *ATP1A2* SHM2/FHM2 causing mutations identified in the C-terminal part of the α2-subunit of the Na^+,K^+-ATPase to investigate the effects of these mutations on the enzyme's apparent Na^+, K^+, and ouabain affinities, as well as maximum ATPase activity and ouabain binding. Baculovirus infected Sf9 insect cells were used to obtain membrane fragments containing the desired mutants. Fig. 2 shows that the amount of protein detected was equal for all mutants compared to wild type enzyme, indicating similar expression levels. As expected, the α-subunit could not be detected in membranes from cells infected with YFP (neg. control).

Subsequently, we investigated protein functionality as reflected by ouabain binding. Ouabain is a well-known and highly specific ligand of Na^+,K^+-ATPase that binds in a pocket constituted by the first six transmembrane spanning domains and specific residues present in several extracellular loops connecting these transmembrane domains

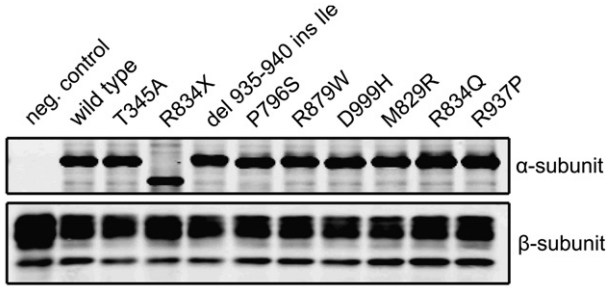

Fig. 2. Western blot showing equal protein expression for all mutants tested in this study. For each mutant, 10 μg of Sf9 membranes was incubated overnight in solubilization buffer and used for SDS-PAGE using 10% acrylamide gels followed by transfer to a nitrocellulose membrane and subsequent detection with antibodies against the α-subunit (C356-M09) and β-subunit (C385-M77). Note that the lower band for mutant R834X (insertion stop codon) reflects a truncated protein, as expected.

[26]. Therefore, binding of ouabain implies that the first six transmembrane domains of Na^+,K^+-ATPase are properly folded. Fig. 3 shows the amount of ouabain binding under equilibrium after incubation with 25 nM radiolabeled ouabain. Wild type, T345A, R879W, R834Q, and R937P membranes showed significantly higher ouabain binding levels compared with control membranes expressing YFP.

Next, we tested the ATPase activity of all mutants by incubation of membranes in the presence of 50 mM NaCl, 5.0 mM KCl, 100 μM ATP and 1.2 mM $MgCl_2$ for 30 min. Table 1 shows that mutants T345A, R834Q and R879W possessed significantly higher ATPase activity than YFP control membranes. We observed that two mutants (R879W and R834Q) showed decreased levels of maximum ATP conversion compared with wild type enzyme: R834Q showed a statistically significant decrease of 78% ($P = 0.03$) and mutant R879W showed a near-significant decrease in ATPase activity of 49%.

Based on the presence of ATPase activity as described above, we tested mutants T345A, R879W and R834Q with regard to their ouabain binding characteristics (Fig. 4, Table 2) and determined the maximum ouabain binding (EO_{max}) as well as ouabain affinities for the different mutants. EO_{max} values ranged from 4.8 pmol/mg for wild type enzyme to 6.3 pmol/mg for T345A, whereas mutants R879W and R834Q showed lower maximum ouabain levels of 2.7 and 0.5 pmol/mg, the latter being significantly decreased when compared with wild type enzyme. The ouabain affinities were identical for wild type and T345A ($K_d = 21 \pm 11$ and 21 ± 6 nM), whereas R879W and R834Q showed non-significant increases in ouabain affinities compared with wild type enzyme ($K_d = 12 \pm 3$ and 12 ± 4 nM).

3.2. Apparent Na^+ and K^+ affinities and turnover numbers

6 out of the 9 mutants possessed no significant ATPase activity (Table 1), providing a hypothesis for their pathogenicity: loss of catalytic activity. However, the lack of ATPase activity also excluded these mutants from further biochemical characterization using ATPase related studies. As a result, we could only determine the Na^+ and K^+ affinities for the remaining three mutants: T345A, R834Q, and R879W (Fig. 5, Table 2).

The apparent Na^+ affinity was studied by investigating the amounts of radioactive ATP hydrolyzed under increasing concentrations of NaCl in the presence of 5.0 mM KCl, 100 μM ATP and 1.2 mM $MgCl_2$. The results of these experiments can be observed in Fig. 5A and Table 2. We observed no significant changes for mutants T345A and R879W compared with wild type, whereas mutant R834Q showed a significant two-fold decrease in apparent Na^+ affinity compared with wild type ($P = 0.0007$).

The apparent K^+ affinity was determined from the amounts of radioactive ATP hydrolyzed under increasing KCl concentrations in the presence of 50 mM NaCl, 100 μM ATP and 1.2 mM $MgCl_2$. The results of these experiments are shown in Fig. 5B and Table 2. There were no significant changes in apparent affinities for T345A and R879W compared with wild type enzyme, whereas mutant R834Q showed a significant two-fold increase in apparent K^+ affinity ($P = 0.013$). This finding is a mirror image of the result observed for the Na^+ affinity of the same mutant, which showed a two-fold decrease in affinity.

By dividing the maximum ATPase activity by the maximum ouabain binding (Table 2), we calculated the turnover number, which is a measure for the specific activity. We did not find any statistically significant differences for the mutants described here (data not shown).

3.3. In silico studies based on homology models

Finally, we performed in silico mutagenesis studies using homology models based on crystal structures of the α1β1 isoform of Na^+,K^+-ATPase as well as the highly similar sarcoplasmatic reticulum Ca^{2+}-ATPase (SERCA). For the three mutants showing ATPase activity, no interactions involving Tyr^{345} and Arg^{879} or their substitutes (alanine and tryptophan, respectively) were predicted, however a hydrogen bond

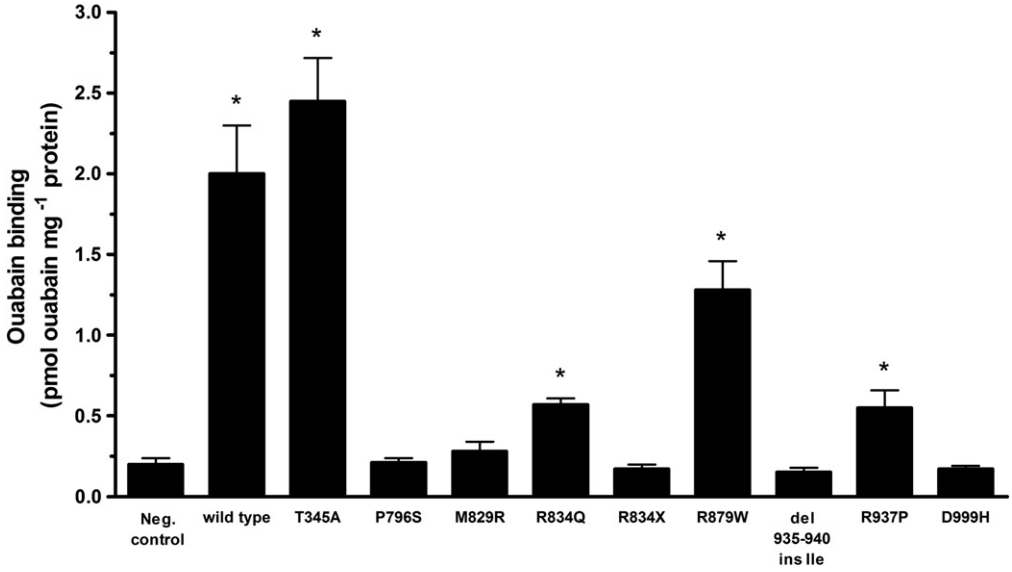

Fig. 3. Amount of bound radiolabeled ouabain for the different mutants. Binding was determined using scintillation counting after 2 h of incubation with 25 nM ouabain at room temperature. Compared to the negative control membranes expressing YFPβ1, wild type and mutants T345A, R834Q, R879W, and R937P showed significantly increased levels of ouabain binding at equilibrium (* = $P < 0.05$ versus neg. control).

network was predicted between residue Arg^{834} and residues Glu^{285} and Glu^{363} in the $E_2.K^+.P_i$ conformation, Asp^{767} in the E_2P conformation, and Asp^{839} in the E_2K^+ ATP conformation (Fig. 6). Regarding the six mutants showing a complete loss of ATPase activity: a hydrogen bond was predicted between serine when introduced at position 796 (P796S) and Arg^{884}, a residue predicted to interact with Gln^{907} as well. Also, introduction of arginine at residue 829 (M829R) led to formation of two hydrogen bonds with Val^{756}.

4. Discussion

We investigated the biochemical characteristics of nine mutations/deletions in the α2-isoform of Na^+,K^+-ATPase linked to sporadic/familial hemiplegic migraine type 2 (SHM2/FHM2) in order to increase our knowledge on the pathogenesis of each of these mutations. All mutants could be expressed in Sf9 insect cells. However, further experiments revealed that six mutants could not be studied in detail due to significant loss of ATPase activity. Three mutants (T345A, R834Q, and R879W) were characterized biochemically, showing significant effects on apparent Na^+- and K^+-affinities for mutant R834Q. Below, we will describe the findings for each mutant and provide hypotheses on how each mutation might lead to the observed effects.

Table 1
Maximum ATPase activity for all mutants studied. Results were obtained by averaging the amount of ATP consumed at 37 °C for 30 min in a medium consisting of 50 mM NaCl, 5.0 mM KCl and 100 μM ATP, corrected for non-specific ATPase activity by incubation of membranes with 1.0 mM ouabain and subsequently background-corrected by subtracting the activity observed for YFPβ1 expressing control membranes.

	Max. ATPase μmol P_i mg^{-1} h^{-1}
Wild type	1.05 ± 0.27
T345A	1.34 ± 0.38
P796S	−0.02 ± 0.03*
M829R	0.00 ± 0.01*
R834Q	0.23 ± 0.05
R834X	−0.03 ± 0.02*
R879W	0.54 ± 0.08
Del 935–940 ins Ile	−0.05 ± 0.01*
R937P	−0.04 ± 0.01*
D999H	−0.02 ± 0.01*

* $P < 0.05$ versus wild type.

T345A was linked to FHM2 in a study describing a Finnish family of which 10 individuals were experiencing FHM attacks, whereas two individuals carried the mutation but most likely did not yet reach the age of onset-of-disease [27]. We did not detect significant changes for any of the parameters tested, although we observed a slightly higher maximum ATPase activity, which was accompanied by a parallel increase in EO_{max}. Although we were not able to identify any interactions of the highly conserved Tyr^{345}, van der Waals' interactions with Val^{362} were hypothesized before [28,29]. Previously, a decreased K^+ affinity and unchanged turnover number were reported for T345A rat cDNA expressed in HeLa cells [30], whereas a study in COS-1 cells showed a reduction in ouabain affinity, an unchanged K^+ affinity, and a decreased turnover number, which were linked to a reduced maximum phosphorylation rate [28]. In contrast to these studies, we used a non-mammalian expression system with two important benefits over the two expression systems mentioned above: the absence of background Na^+,K^+-ATPase as well as equimolar expression of the α- and β-subunits. The differences between these expression systems might provide explanations for the differences between these studies and our results.

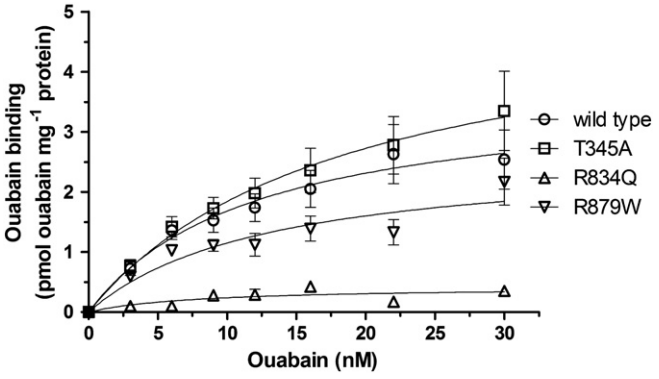

Fig. 4. Ouabain binding characteristics of mutants T345A, R834Q, and R879W and wild type enzyme. Membranes were incubated with different concentrations of radiolabeled ouabain at room temperature for 2 h, followed by filtration over ME-27 filters. Radioactivity retained on the filters, containing the enzyme–ouabain complex, was subsequently quantified using liquid scintillation analysis.

Table 2
Characteristics of ATPase activity and ouabain binding for wild type, T345A, R834Q and R879W enzymes. ATPase experiments using radiolabeled ATP were performed to determine apparent Na^+ and K^+ affinities and maximum ATPase values, whereas radiolabeled ouabain was used to determine apparent ouabain affinity and maximum binding level.

	ATPase activity			Ouabain binding	
	Max. ATPase μmol P_i mg^{-1} h^{-1}	$Na^+_{0.5}$ mM	$K^+_{0.5}$ mM	Max. binding pmol/mg protein	Affinity nM
Wild type	1.05 ± 0.3	5.9 ± 0.2	1.10 ± 0.1	4.80 ± 1.2	21.0 ± 10.4
T345A	1.34 ± 0.4	6.2 ± 0.2	1.30 ± 0.1	6.30 ± 2.1	21.0 ± 6.3
R834Q	0.23 ± 0.1*	11.6 ± 0.4*	0.50 ± 0.1*	0.50 ± 0.0*	11.8 ± 4.0
R879W	0.54 ± 0.1	6.5 ± 0.3	1.00 ± 0.0	2.70 ± 0.4	11.9 ± 3.0
		nH = 2.03	nH = 1.93		nH = 1.00

nH = Hill coefficient.
* $P < 0.05$ versus wild type.

The R834Q mutation was discovered in a French family containing eleven individuals suffering from FHM [31]. We identified a significantly decreased apparent Na^+ affinity, increased apparent K^+ affinity, and decreased maximum ATPase activity and maximum ouabain binding compared to wild type enzyme. An increase in apparent K^+ affinity has been reported before [28], but we are the first to report a decrease in apparent Na^+ affinity for this mutation. Based on the lower maximum ATPase activity, re-uptake of K^+ from the synaptic cleft might be decreased, although an increased apparent K^+ affinity could diminish this effect. As predicted by the homology models used in this study, Arg^{834} is involved in interactions with other residues present in the cytosolic domains of Na^+,K^+-ATPase, serving an important role in interactions between different domains during the catalytic cycle as pointed out before [32]. Being located in the cytosolic loop between the sixth and seventh transmembrane domains (αM6–αM7), Arg^{834} is also part of the C-terminal half-channel, serving as a gateway to the third ion-binding site by allowing protons to access this site as required for K^+ occlusion [17]. We hypothesize that substitution of Arg^{834} with a glutamine (resulting in removal of a positive charge at this residue) disturbs hydrogen bond interaction networks shown in Fig. 6, thereby affecting the structure and/or accessibility of the C-terminal half-channel, interfering indirectly with apparent Na^+ and K^+ affinities and the transitions between different conformations.

Mutation R879W was found in a screen for mutations in patients suffering from sporadic hemiplegic migraine (SHM) and was identified together with another mutation of the same non-conserved residue, R879Q [33]. Although no mutations were detected in 92 controls, both *ATP1A2* mutations were also found in non-affected family members, questioning the dominance in SHM. Our data seem to confirm this lack of causality, as they show a non-significant increase in ouabain affinity as well as a non-significant decrease in apparent maximum ATPase activity compared to wild type enzyme. Based on analysis of different homology models, we were not able to identify any hydrogen bond interacting residues for Arg^{879}, in line with the low conservation of this residue among different isoforms. Previously, we reported on another mutation at the same position (R879Q), which showed only minor changes in the enzyme's biochemical properties, leading us to conclude that this mutation might not be pathogenic [19]. Here, we conclude the same for R879W, strengthening our hypothesis that there is no link to SHM for mutations involving Arg^{879}.

Mutation P796S was linked to FHM2 in a Portuguese family by a cell assay that showed no survival of HeLa cells transfected with the mutated Na^+,K^+-ATPase, inferring pathogenicity for this mutation [29]. Introduction of serine resulted in prediction of a hydrogen bond with Arg^{884}, which in turn is involved in a hydrogen bond with Gln^{907}, located in the C-terminal half of the extracellular loop between αM7 and αM8, implicated in interactions between the α- and β-subunits [34]. Possibly, substitution of proline with serine results in affected interactions between both subunits leading to a complete loss of ATPase activity as observed here, or might result in improper insertion of the enzyme into the membrane due to loss of these interactions.

M829R was identified in a study describing multiple new mutations linked to FHM2 [31] and subsequently reported to result a minor increase in apparent K^+ affinity in oocytes [32]. Our study shows a complete loss of ATPase activity for this mutant, implying an even more severe effect of this mutation. Again, the difference in experimental results might be related to the insect cells used here, which are cultured at 27 °C instead of 18 °C used for oocytes. Based on analysis of the first crystal structure of the Na^+,K^+-ATPase [35], the highly conserved Met^{829} has been implicated in important interactions stabilizing the interdomain interface region between αM6 and αM7 during the catalytic cycle [32]. Therefore, it is likely that replacement of methionine with arginine results in disturbance of these essential hydrogen bond networks, leading to loss of ATPase activity as shown here.

The mutations R834X [36], del 935–940 ins Ile [31], R937P [31] and D999H [37], all showing complete loss of ATPase activity, affect one or more residues involved in the structure of the C-terminal pathway. This half-channel controls the access of protons from the cytosol to the third proposed ion-binding site and plugs this channel upon occlusion of the third ion binding site (IIIb) by either Na^+ (E_1 state) or H^+ (E_2 state) [17]. Disruption of this half-channel could therefore easily lead to loss of ATPase activity resulting from the absence of Na^+ and K^+ occlusion, in particular for the mutations affecting multiple residues of the C-terminal segment including R834X (insertion stop codon) and

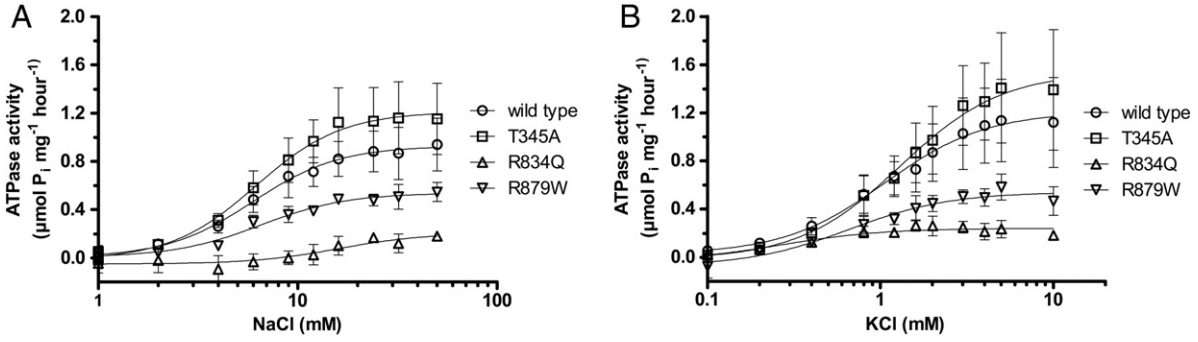

Fig. 5. Average ($n \geq 3$) background corrected Na^+ (A) and K^+ (B) ATPase activities for wild type, T345A, R834Q and R879W enzymes. ATPase activities were determined by measuring the amount of radioactive ATP hydrolyzed after incubation of membranes for 30 min at 37 °C under different concentrations of either NaCl (A) or KCl (B).

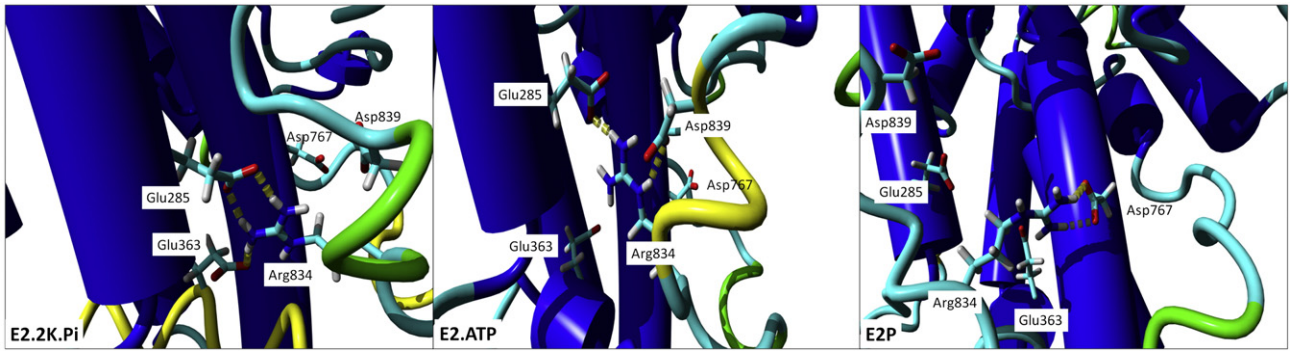

Fig. 6. Conformation dependent hydrogen bond interactions between Arg^{834} and various other amino acids that take place during the Na^+,K^+-ATPase reaction cycle. Arg^{834} is predicted to interact with Glu^{285} and Glu^{363} in the $E_2.2K^+.P_i$ conformation (homology model based on 2ZXE), Asp^{767} in the E_2P conformation (homology model based on 3B9B), and Asp^{839} in the E_2K^+ ATP conformation (homology model based on 2C88).

del 935–940 in. Ile. Arg^{937} was found to play a role in controlling the C-terminal tyrosine residues essential for ATPase activity by forming hydrogen bonds and cation–π interactions [17]. The same study also described Asp^{999} as one of the residues facing inwards into the proposed channel, highlighting the importance of this residue for ATPase activity as well. We hypothesize that mutation of this residue into a positively charged histidine disturbs C-terminal function, interfering with the affinity and occlusion of Na^+ and/or H^+, thereby indirectly affecting ATPase function.

In conclusion, we found a statistically significant decrease in maximum ATPase activity and apparent K^+ affinity together with an increase in apparent Na^+ affinity for mutation R834Q. Mutants T345A and R879W did not show any significant changes for the parameters studied here. Mutants P796S, M829R, R834X, del 935–940 ins Ile, R937P and D999H could not be tested due to a lack of ATPase activity, but this might explain how these mutations, as well as R834Q, lead to development of SHM2/FHM2 by affecting transport of K^+ and Na^+ between the synaptic cleft and supporting cells expressing the α2-isoform of Na^+, K^+-ATPase. Lack of transport of Na^+ and K^+ is believed to affect the secondary active transport of glutamate eventually leading to decreased recovery from neural excitation associated with development of SHM2/FHM2 attacks.

Supplementary data to this article can be found online at http://dx.doi.org/10.1016/j.bbamem.2014.03.022.

Acknowledgements

Financial support for this study was provided by a personal VIDI grant (700.58.427) from the Netherlands Organisation for Scientific Research to J.B.K. There was no involvement of the funding source with any part of the research performed or decision to submit this article.

References

[1] R. Whittam, J.S. Willis, Ion movements and oxygen consumption in kidney cortex slices, J. Physiol. 168 (1963) 158–177.
[2] J.C. Skou, Nobel lecture. The identification of the sodium pump, Biosci. Rep. 18 (1998) 155–169.
[3] W. Kuhlbrandt, Biology, structure and mechanism of P-type ATPases, Nat. Rev. Mol. Cell Biol. 5 (2004) 282–295.
[4] A.Y. Bagrov, J.I. Shapiro, O.V. Fedorova, Endogenous cardiotonic steroids: physiology, pharmacology, and novel therapeutic targets, Pharmacol. Rev. 61 (2009) 9–38.
[5] G. Blanco, R.W. Mercer, Isozymes of the Na–K-ATPase: heterogeneity in structure, diversity in function, Am. J. Physiol. 275 (1998) F633–F650.
[6] O.I. Shamraj, J.B. Lingrel, A putative fourth Na+, K(+)-ATPase alpha-subunit gene is expressed in testis, Proc. Natl. Acad. Sci. U. S. A. 91 (1994) 12952–12956.
[7] V. Hieber, G.J. Siegel, D.J. Fink, M.W. Beaty, M. Mata, Differential distribution of (Na, K)-ATPase alpha isoforms in the central nervous system, Cell. Mol. Neurobiol. 11 (1991) 253–262.
[8] D. Romanovsky, A.E. Moseley, R.E. Mrak, M.D. Taylor, M. Dobretsov, Phylogenetic preservation of alpha3 Na+, K+-ATPase distribution in vertebrate peripheral nervous systems, J. Comp. Neurol. 500 (2007) 1106–1116.
[9] K.M. McGrail, J.M. Phillips, K.J. Sweadner, Immunofluorescent localization of three Na,K-ATPase isozymes in the rat central nervous system: both neurons and glia can express more than one Na,K-ATPase, J. Neurosci. Off. J. Soc. Neurosci. 11 (1991) 381–391.
[10] B. de Vries, R.R. Frants, M.D. Ferrari, A.M. van den Maagdenberg, Molecular genetics of migraine, Hum. Genet. 126 (2009) 115–132.
[11] M.B. Russell, A. Ducros, Sporadic and familial hemiplegic migraine: pathophysiological mechanisms, clinical characteristics, diagnosis, and management, Lancet Neurol. 10 (2011) 457–470.
[12] L.L. Thomsen, M.K. Eriksen, S.F. Roemer, I. Andersen, J. Olesen, M.B. Russell, A population-based study of familial hemiplegic migraine suggests revised diagnostic criteria, Brain 125 (2002) 1379–1391.
[13] L.L. Thomsen, E. Ostergaard, J. Olesen, M.B. Russell, Evidence for a separate type of migraine with aura: sporadic hemiplegic migraine, Neurology 60 (2003) 595–601.
[14] D. Pietrobon, Familial hemiplegic migraine, Neurotherapeutics 4 (2007) 274–284.
[15] P. Bottger, C. Doganli, K. Lykke-Hartmann, Migraine- and dystonia-related disease-mutations of Na+/K+-ATPases: relevance of behavioral studies in mice to disease symptoms and neurological manifestations in humans, Neurosci. Biobehav. Rev. 36 (2012) 855–871.
[16] J.P. Morth, B.P. Pedersen, M.J. Buch-Pedersen, J.P. Andersen, B. Vilsen, M.G. Palmgren, P. Nissen, A structural overview of the plasma membrane Na+, K+-ATPase and H+-ATPase ion pumps, Nat. Rev. Mol. Cell Biol. 12 (2011) 60–70.
[17] H. Poulsen, H. Khandelia, J.P. Morth, M. Bublitz, O.G. Mouritsen, J. Egebjerg, P. Nissen, Neurological disease mutations compromise a C-terminal ion pathway in the Na(+)/K(+)-ATPase, Nature 467 (2010) 99–102.
[18] V.A. Luckow, S.C. Lee, G.F. Barry, P.O. Olins, Efficient generation of infectious recombinant baculoviruses by site-specific transposon-mediated insertion of foreign genes into a baculovirus genome propagated in *Escherichia coli*, J. Virol. 67 (1993) 4566–4579.
[19] H.G. Swarts, K.M. Weigand, H. Venselaar, A.M. van den Maagdenberg, F.G. Russel, J.B. Koenderink, Familial hemiplegic migraine mutations affect Na,K-ATPase domain interactions, Biochim. Biophys. Acta 1832 (2013) 2173–2179.
[20] A.A. El-Sheikh, J.J. van den Heuvel, E. Krieger, F.G. Russel, J.B. Koenderink, Functional role of arginine 375 in transmembrane helix 6 of multidrug resistance protein 4 (MRP4/ABCC4), Mol. Pharmacol. 74 (2008) 964–971.
[21] H.G. Swarts, J.B. Koenderink, P.H. Willems, J.J. De Pont, The non-gastric H, K-ATPase is oligomycin-sensitive and can function as an H+, NH_4(+)-ATPase, J. Biol. Chem. 280 (2005) 33115–33122.
[22] G.L. Peterson, Determination of total protein, Methods Enzymol. 91 (1983) 95–119.
[23] J.B. Koenderink, S. Geibel, E. Grabsch, J.J. De Pont, E. Bamberg, T. Friedrich, Electrophysiological analysis of the mutated Na,K-ATPase cation binding pocket, J. Biol. Chem. 278 (2003) 51213–51222.
[24] L.Y. Qiu, J.B. Koenderink, H.G. Swarts, P.H. Willems, J.J. De Pont, Phe783, Thr797, and Asp804 in transmembrane hairpin M5–M6 of Na+, K+-ATPase play a key role in ouabain binding, J. Biol. Chem. 278 (2003) 47240–47244.
[25] J.B. Koenderink, H.G. Swarts, H.P. Hermsen, J.J. De Pont, The beta-subunits of Na+, K+-ATPase and gastric H+, K+-ATPase have a high preference for their own alpha-subunit and affect the K+ affinity of these enzymes, J. Biol. Chem. 274 (1999) 11604–11610.
[26] L.Y. Qiu, E. Krieger, G. Schaftenaar, H.G. Swarts, P.H. Willems, J.J. De Pont, J.B. Koenderink, Reconstruction of the complete ouabain-binding pocket of Na,K-ATPase in gastric H, K-ATPase by substitution of only seven amino acids, J. Biol. Chem. 280 (2005) 32349–32355.
[27] M.A. Kaunisto, H. Harno, K.R. Vanmolkot, J.J. Gargus, G. Sun, E. Hamalainen, E. Liukkonen, M. Kallela, A.M. van den Maagdenberg, R.R. Frants, M. Farkkila, A. Palotie, M. Wessman, A novel missense ATP1A2 mutation in a Finnish family with familial hemiplegic migraine type 2, Neurogenetics 5 (2004) 141–146.
[28] V.R. Schack, R. Holm, B. Vilsen, Inhibition of phosphorylation of Na+, K+-ATPase by mutations causing familial hemiplegic migraine, J. Biol. Chem. 287 (2012) 2191–2202.
[29] M.J. Castro, B. Nunes, B. de Vries, C. Lemos, K.R. Vanmolkot, J.J. van den Heuvel, T. Temudo, J. Barros, J. Sequeiros, R.R. Frants, J.B. Koenderink, J.M. Pereira-Monteiro, A.M. van den Maagdenberg, Two novel functional mutations in the Na+, K+-ATPase alpha2-subunit ATP1A2 gene in patients with familial hemiplegic migraine and associated neurological phenotypes, Clin. Genet. 73 (2008) 37–43.

[30] L. Segall, R. Scanzano, M.A. Kaunisto, M. Wessman, A. Palotie, J.J. Gargus, R. Blostein, Kinetic alterations due to a missense mutation in the Na,K-ATPase alpha2 subunit cause familial hemiplegic migraine type 2, J. Biol. Chem. 279 (2004) 43692–43696.
[31] F. Riant, F.M. De, P. Aridon, A. Ducros, C. Ploton, F. Marchelli, J. Maciazek, M.G. Bousser, G. Casari, E. Tournier-Lasserve, ATP1A2 mutations in 11 families with familial hemiplegic migraine, Hum. Mutat. 26 (2005) 281.
[32] N.N. Tavraz, T. Friedrich, K.L. Durr, J.B. Koenderink, E. Bamberg, T. Freilinger, M. Dichgans, Diverse functional consequences of mutations in the Na+/K+-ATPase alpha2-subunit causing familial hemiplegic migraine type 2, J. Biol. Chem. 283 (2008) 31097–31106.
[33] L.L. Thomsen, E. Oestergaard, A. Bjornsson, H. Stefansson, A.C. Fasquel, J. Gulcher, K. Stefansson, J. Olesen, Screen for CACNA1A and ATP1A2 mutations in sporadic hemiplegic migraine patients, Cephalalgia 28 (2008) 914–921.
[34] M.V. Lemas, M. Hamrick, K. Takeyasu, D.M. Fambrough, 26 amino acids of an extracellular domain of the Na,K-ATPase alpha-subunit are sufficient for assembly with the Na,K-ATPase beta-subunit, J. Biol. Chem. 269 (1994) 8255–8259.
[35] J.P. Morth, B.P. Pedersen, M.S. Toustrup-Jensen, T.L. Sorensen, J. Petersen, J.P. Andersen, B. Vilsen, P. Nissen, Crystal structure of the sodium–potassium pump, Nature 450 (2007) 1043–1049.
[36] B. de Vries, T. Freilinger, K.R. Vanmolkot, J.B. Koenderink, A.H. Stam, G.M. Terwindt, E. Babini, E.H. van den Boogerd, J.J. van den Heuvel, R.R. Frants, J. Haan, M. Pusch, A.M. van den Maagdenberg, M.D. Ferrari, M. Dichgans, Systematic analysis of three FHM genes in 39 sporadic patients with hemiplegic migraine, Neurology 69 (2007) 2170–2176.
[37] D.M. Fernandez, C.K. Hand, B.J. Sweeney, N.A. Parfrey, A novel ATP1A2 gene mutation in an Irish familial hemiplegic migraine kindred, Headache 48 (2008) 101–108.
[38] T. Shinoda, H. Ogawa, F. Cornelius, C. Toyoshima, Crystal structure of the sodium–potassium pump at 2.4 A resolution, Nature 459 (2009) 446–450.